frontiers | Frontiers in Endocrinology

TYPE Original Research
PUBLISHED 12 October 2023
DOI 10.3389/fendo.2023.1212854

OPEN ACCESS

EDITED BY
Nandini Vasudevan,
University of Reading, United Kingdom

REVIEWED BY
Susan Wray,
National Institute of Neurological Disorders and Stroke (NIH), United States
Shunji Yamada,
Kyoto Prefectural University of Medicine, Japan

*CORRESPONDENCE
Richard Piet
rpiet@kent.edu

RECEIVED 27 April 2023
ACCEPTED 19 September 2023
PUBLISHED 12 October 2023

CITATION
Buo C, Bearss RJ, Novak AG, Anello AE, Dakin JJ and Piet R (2023) Serotonin stimulates female preoptic area kisspeptin neurons *via* activation of type 2 serotonin receptors in mice. *Front. Endocrinol.* 14:1212854. doi: 10.3389/fendo.2023.1212854

Serotonin stimulates female preoptic area kisspeptin neurons *via* activation of type 2 serotonin receptors in mice

Carrie Buo[1], Robin J. Bearss[1,2], Alyssa G. Novak[1], Anna E. Anello[1], Jordan J. Dakin[1] and Richard Piet[1,2]*

[1]Brain Health Research Institute and Department of Biological Sciences, Kent State University, Kent, OH, United States, [2]School of Biomedical Sciences, Kent State University, Kent, OH, United States

Background: The neuroendocrine control of ovulation is orchestrated by neuronal circuits that ultimately drive the release of gonadotropin-releasing hormone (GnRH) from the hypothalamus to trigger the preovulatory surge in luteinizing hormone (LH) secretion. While estrogen feedback signals are determinant in triggering activation of GnRH neurons, through stimulation of afferent kisspeptin neurons in the rostral periventricular area of the third ventricle ($RP3V^{KISS1}$ neurons), many neuropeptidergic and classical neurotransmitter systems have been shown to regulate the LH surge. Among these, several lines of evidence indicate that the monoamine neurotransmitter serotonin (5-HT) has an excitatory, permissive, influence over the generation of the surge, *via* activation of type 2 5-HT ($5\text{-}HT_2$) receptors. The mechanisms through which this occurs, however, are not well understood. We hypothesized that 5-HT exerts its influence on the surge by stimulating $RP3V^{KISS1}$ neurons in a $5\text{-}HT_2$ receptor-dependent manner.

Methods: We tested this using kisspeptin neuron-specific calcium imaging and electrophysiology in brain slices obtained from male and female mice.

Results: We show that exogenous 5-HT reversibly increases the activity of the majority of $RP3V^{KISS1}$ neurons. This effect is more prominent in females than in males, is likely mediated directly at $RP3V^{KISS1}$ neurons and requires activation of $5\text{-}HT_2$ receptors. The functional impact of 5-HT on $RP3V^{KISS1}$ neurons, however, does not significantly vary during the estrous cycle.

Conclusion: Taken together, these data suggest that $5\text{-}HT_2$ receptor-mediated stimulation of $RP3V^{KISS1}$ neuron activity might be involved in mediating the influence of 5-HT on the preovulatory LH surge.

KEYWORDS

hypothalamus, GnRH neuronal network, preovulatory surge, GCaMP-based calcium imaging, action potential firing

1 Introduction

Fertility in all mammals is ultimately controlled by gonadotropin-releasing hormone (GnRH) neurons, which drive the release of anterior pituitary gland gonadotropins luteinizing hormone (LH) and follicle-stimulating hormone. In females of spontaneously ovulating species, the rise in circulating estrogen (E) concentration stimulates the mid-cycle surge in GnRH and LH secretion that causes ovulation (1). Because GnRH neurons do not express E receptor α (ERα), the receptor required for the preovulatory surge (2–6), these cells rely on afferent ERα-expressing neurons, the GnRH neuronal network, to relay E feedback information (7). An important part of this network for mediating preovulatory E positive feedback is the preoptic area (POA) subpopulation of kisspeptin (KISS1) neurons found in two contiguous nuclei – the anteroventral periventricular nucleus and the periventricular nucleus – referred to together as the rostral periventricular area of the third ventricle (RP3V) (8, 9). RP3V^{KISS1} neurons express ERα, undergo physiological changes in response to E positive feedback, project to GnRH neurons and can drive GnRH neuron action potential firing and surge-like LH secretion [reviewed in (10–12)].

Although E positive feedback is an obligatory determinant of the preovulatory surge in spontaneous ovulators (1), many other cues regulate this neuroendocrine event through actions of neuropeptides and neurotransmitters on the GnRH neuronal network [for reviews see (7, 13–22)]. Among these, many lines of evidence indicate that the monoamine neurotransmitter serotonin (5-hydroxytryptamine, 5-HT) plays a role in the LH surge in rodents. Lesions of the dorsal raphe nucleus (DR), which comprises 5-HT-producing neurons, inhibit the LH surge (23–26). Further suggesting a role for endogenously released 5-HT, depletion of 5-HT and 5-HT receptor antagonism both suppress the LH surge (24, 27–31). Moreover, blockade of type 2 5-HT (5-HT$_2$) receptors prevents the surge (32–34) while activation of 5-HT$_2$ receptors is sufficient to restore the surge in animals with a DR lesion (26), indicating that 5-HT$_2$ receptors might play a central role.

The mechanisms through which 5-HT might regulate the LH surge, however, are not fully understood. While evidence suggests that 5-HT neurons might influence the surge *via* indirect mechanisms (35–37), a direct influence on the GnRH neuronal network may also be at play. Indeed, 5-HT neuronal fibers are found in the RP3V (38–40) as well as in the vicinity of GnRH neurons in the POA (41), some of which originate in the DR (42). These projections might be important seeing that 5-HT release in the hypothalamus, including the POA, increases during the surge and that neurotoxic lesion of 5-HT neuron fibers in the POA prevents the surge (28, 43). At the cellular level, 5-HT can increase or decrease action potential firing and GnRH release *via* activation of multiple 5-HT receptors in immortalized GnRH neurons maintained in culture (44, 45). Some of these effects are seen in native GnRH neurons recorded in brain slices, where, curiously, most (≈75%) female GnRH neurons are inhibited by 5-HT, *via* a 5-HT$_1$ receptor-mediated mechanism, whereas only a subset exhibits 5-HT$_2$ receptor-mediated increases in activity (46). The impact of 5-HT neurotransmission on the LH surge, therefore, cannot be fully accounted for by effects of this neurotransmitter on GnRH neurons.

We hypothesized here that the impact of 5-HT on the LH surge is mediated, at least in part, through regulation of RP3V^{KISS1} neurons upstream of GnRH neurons. Using GCaMP-based calcium imaging and electrophysiology in brain slices, we investigated the effect of 5-HT on RP3V^{KISS1} neuron activity and the role of 5-HT$_2$ receptors therein.

2 Materials and methods

2.1 Animals

Mice expressing the genetically encoded calcium indicator GCaMP6f (47) in kisspeptin neurons were generated by crossing mice that express the Cre recombinase enzyme (Cre) in kisspeptin cells (Kiss1-Cre; Jackson laboratory stock #023426) (48) with mice that express Cre-dependent GCaMP6f at the ROSA26 locus (flox-STOP-GCaMP6f; Jackson laboratory stock #028865) (49). Male and female offspring heterozygous for the Kiss1-Cre and flox-STOP-GCaMP6f alleles (Kiss1-Cre::GCaMP6f) were used in calcium imaging experiments. Female mice expressing the humanized *renilla* green fluorescent protein (hrGFP) in kisspeptin neurons (Kiss1-hrGFP; Jackson laboratory stock #023426) (50) were used in electrophysiology experiments. All experimental mice were adults (2-6 months). Female estrous cycle stage was determined by vaginal lavage (5 µL H_2O) taken between zeitgeber time (ZT) 1 and 3 or *post-mortem* (ZT2.5-5.5). Aqueous vaginal smears were stained with methylene blue and cytology examined under light microscopy to assess estrous cycle stage (51). Mice were group-housed with littermates under controlled temperature (23 ± 2°C) and lighting (12h light/dark) conditions with *ad libitum* access to food and water. Mice were assigned to experiments based on their genotype, sex, and on their estrous cycle stage as needed. All experiments were approved by Kent State University's Institutional Animal Care and Use Committee.

2.2 Fixed brain slice preparation and imaging

To visualize the distribution of GCaMP6f-expressing neurons in the RP3V of male and female mice, two male and two female (one diestrus and one proestrus) Kiss1-Cre::GCaMP6f mice were deeply anesthetized *via* intraperitoneal injection of 3 mg/mL pentobarbital before being perfused through the heart with 4% paraformaldehyde (PFA). The brains were then dissected out and placed in 4% PFA for 1 hour before being transferred to 20% sucrose in 0.1 M phosphate-buffered saline. The brains were then cut in 3 series of coronal sections (30 µm thick) using a freezing microtome. The tissue was mounted onto superfrost charged slices, air dried, and coverslipped using an aqueous mounting medium (ProLong™ Gold antifade mountant, Thermofisher). Epifluorescence images were taken in the

RP3V region using a DMR microscope (Leica Microsystems) equipped with an ORCA-FLASH 4.0 V3 Digital CMOS (Hamamatsu, Japan), controlled by the MicroBrightField Neurolucida Software (MBF Bioscience).

2.3 Live brain slice preparation

Brain slices were prepared as previously described (52, 53). Briefly, mice were decapitated following isoflurane anesthesia, and their brains quickly removed. Coronal brain slices (200 µm thick) containing the RP3V were cut using a vibrating blade microtome (HM650V, Microm International GmbH) in an ice-cold solution containing (in mM): 87 NaCl, 2.5 KCl, 25 $NaHCO_3$, 1.25 NaH_2PO_4, 0.5 $CaCl_2$, 6 $MgCl_2$, 25 glucose and 75 sucrose. Brain slices were left to incubate at 30-34°C for at least 1 hour in artificial cerebrospinal fluid (aCSF) containing (in mM): 125 NaCl, 2.5 KCl, 26 $NaHCO_3$, 1.25 NaH_2PO_4, 2.5 $CaCl_2$, 1.2 $MgCl_2$ and 11 glucose. All solutions were equilibrated to pH 7.4 with a mixture of 95% O_2/5% CO_2. Female mice were killed between ZT2.5 and 5.5 and males between ZT2 and 4.5.

2.4 Calcium imaging and electrophysiology

Individual brain slices obtained from Kiss1-Cre::GCaMP6f or Kiss1-hrGFP mice were placed under an upright epifluorescence microscope (either Scientifica, UK or Prior Scientific, UK) and constantly perfused (1.5 mL/min) with warm (32-34°C) aCSF.

Variations in intracellular calcium concentration ($[Ca^{2+}]_i$) in $RP3V^{KISS1}$ neurons were estimated by measuring fluorescence changes in individual GCaMP6f-expressing RP3V neurons in slices from Kiss1-Cre::GCaMP6f mice. Slices were illuminated through a 40x immersion objective, using a light-emitting diode light source ($pE300^{ultra}$ LED; CoolLED, UK) filtered for blue light excitation (460-487 nm; Semrock, USA). Epifluorescence (emission 500-546 nm; Semrock, USA) was collected using an ORCA-FLASH 4.0 LT+ CMOS camera (Hamamatsu). LED and camera were controlled and synchronized with the µ-manager 1.4 software (54). After a ≥15-minute stabilization period in the recording chamber, a focal plane including several fluorescent cell bodies was chosen and acquisitions (100 ms light exposure at 2 Hz for 10-15 minutes) started. Low intensity LED illumination was used (≈0.1 to 0.8 mW) to minimize GCaMP6f photobleaching.

$RP3V^{KISS1}$ neuron spontaneous action potential firing was recorded in brain slices from Kiss1-hrGFP mice. GFP-expressing RP3V neurons were visualized using brief LED illumination (excitation and emission as above) and subsequently approached with glass recording micropipettes using infrared differential interference contrast illumination. Recording micropipettes (tip resistance: 3-6 MΩ) were made with borosilicate glass (cat. #BF150-110-7.5, Sutter Instruments, USA), pulled using a Model P-1000 micropipette puller (Sutter Instruments). Action potential firing was recorded in voltage-clamp mode (no holding potential applied) in the minimally invasive cell-attached configuration (12-30 MΩ initial seal resistance). Glass micropipettes were filled with aCSF and the recording configuration was achieved by applying the lowest amount of suction required to detect spontaneous, fast, downward deflections in the current trace (spikes), which correspond to single action potentials (55). Electrical signals were recorded, filtered at 2 kHz, and digitized at 10 to 20 kHz using a double integrated patch amplifier (Sutter Instruments, USA), and acquired with the SutterPatch software (Sutter Instruments, USA).

All calcium imaging and electrophysiology experiments were performed between ZT3.5 and 10.

2.5 Drug applications

All drugs were dissolved to the appropriate stock concentration in water or in DMSO, aliquoted and stored at -20°C. Stock were diluted to working concentrations in aCSF prior to performing experiments. Final DMSO concentration never exceeded 0.1%. All drugs were bath-applied. Agonists were applied for one or two minutes after a ≥ three-minute baseline period in electrophysiology and in calcium imaging experiments. Antagonists and blockers were applied continuously to the slice for ≥ five minutes before a recording started and for the duration of the recording. In calcium imaging experiments, cell viability was routinely tested at the end of the experiments by applying the glutamate receptor agonists (S)-α-Amino-3-hydroxy-5-methyl-4-isoxazolepropionic acid (AMPA; 10-20 µM) or L-glutamate (100 µM), or by raising extracellular $[K^+]$ (+ 10 mM KCl).

AMPA (cat. #0254), the 5-HT_2 receptor antagonists 6-[2-[4-[Bis(4-fluorophenyl)methylene]-1-piperidinyl]ethyl]-7-methyl-5H-thiazolo [3,2-a]pyrimidin-5-one (ritanserin; cat. #1955) and 1,2,3,4,10,14b-Hexahydro-2-methyldibenzo[c,f]pyrazino[1,2-a]azepine hydrochloride (mianserin; cat. #0997), the 5-HT_{2A} receptor agonist (4-Bromo-3,6-dimethoxybenzocyclobuten-1-yl)methylamine hydrobromide (TCB-2; cat. #2592), the 5-HT_{2C} receptor agonist 8,9-Dichloro-2,3,4,4a-tetrahydro-1*H*-pyrazino[1,2-a]quinoxalin-5(6*H*)-one hydrochloride (WAY161503; cat. #1801), the 5-HT_3 receptor agonist 1-(6-Chloro-2-pyridinyl)-4-piperidinamine hydrochloride (SR57227; cat. #1205), the 5-HT_4 receptor agonist (±)-4-Amino-5-chloro-*N*-[1-[(3R*,4S*)-3-(4-fluorophenoxy)propyl]-3-methoxy-4-piperidinyl]-2-methoxybenzamide (cisapride; cat. #1695), the 5-HT_6 receptor agonist 3-[(-3-Fluorophenyl)sulfonyl]-*N*,*N*-dimethyl-1*H*-pyrrolo[2,3-*b*]pyridine-1-ethanamine dihydrochloride (WAY208466; cat. #3904), the 5-HT_7 receptor agonist (2*S*)-5-(1,3,5-Trimethylpyrazol-4-yl)-2-(dimethylamino)tetralin (AS19; cat. #1968) and 5-HT hydrochloride (cat. #3547) were purchased from Tocris (Bio-techne, USA). L-glutamate (cat. #HB0383) was purchased from HelloBio (USA) and tetrodotoxin citrate (cat. #T-550) from Alomone labs (Israel).

2.6 Analysis

For calcium imaging, GCaMP6ffluorescence image time-series were processed in the FIJI software (56). Regions of interest (ROIs) were drawn around individual, in-focus fluorescent somata [12.1 ± 0.5 (ranging 4 to 24) and 9.2 ± 1.0 (ranging 7 to 14) ROIs per slice in females and males, respectively]. Mean fluorescence intensity within

each ROI was measured in each frame. Fluorescence intensity data were analyzed using scripts written in R (http://www.r-project.org/). For each ROI, normalized fluorescence was calculated as $\frac{Ft}{F} \times 100$, where F is the baseline fluorescence intensity calculated as the mean fluorescence intensity over a one-minute period preceding agonist applications and F_t is the fluorescence measured at any time point. Time-dependent bleaching was corrected by subtracting the normalized fluorescence obtained in an ROI that did not contain a fluorescent cell within the RP3V (empty ROI). This approach could not be used for recordings of the effect of AMPA, L-glutamate or KCl as these treatments induced very large increases in fluorescence that contaminated the empty ROI, thereby causing unacceptable distortions of traces upon subtraction. ROIs in which normalized fluorescence traces reversibly increased from baseline for a period of at least 2 minutes, around the time of agonist application, were recorded as being excited. For illustration and statistical comparisons, agonist effects were calculated as the mean normalized fluorescence over 30 seconds at the peak of the effect minus that over 30 seconds of baseline.

For electrophysiology, spikes were detected using the threshold crossing method. Spike time stamps were organized into ten-second bins and the mean firing rate calculated for each bin. To determine if 5-HT affected the spontaneous firing of RP3V^{KISS1} neurons, baseline firing was first measured as the mean firing rate during the two minutes preceding 5-HT application. Recordings in which the mean firing rate changed by greater than twice the standard deviation of baseline (2 × SD) during the five minutes after 5-HT first entered the bath were recorded as displaying a response to 5-HT. For statistical comparisons, firing rates were averaged over a one-minute period during baseline and at the peak of 5-HT effect.

In total, 800 GCaMP6f-expressing cells in 64 slices from 45 female mice and 55 GCaMP6f-expressing cells in 6 slices from 5 male mice were analyzed in calcium imaging experiments, while 17 GFP-expressing cells in 11 slices from 7 female mice were analyzed in electrophysiology experiments. These numbers are broken down by experiments in the results section.

Statistical analyses were performed using Prism 9.0 (GraphPad, USA). Data are reported in the text and tables as mean ± SEM, and in figures as mean ± SEM or ± 95% confidence intervals. Comparisons between two independent groups were made using the Mann-Whitney test and those between two paired groups using the paired t-test or the Wilcoxon signed rank test, as appropriate. Comparisons between multiple groups were made with the Kruskal-Wallis test with Dunn's post-tests. Comparisons of proportions were made using Fisher's exact tests. Differences were considered statistically significant for $p < 0.05$.

3 Results

3.1 5-HT stimulates RP3V^{KISS1} neuron activity in a sex-dependent, but not estrous cycle-dependent, manner

The effects of 5-HT on RP3V^{KISS1} neuron activity were assessed using calcium imaging in brain slices from male and female Kiss1-Cre::GCaMP6f mice (Figures 1A, B). In slices from female mice, two-minute bath applications of 5-HT (10 µM) resulted in transient increases in GCaMP6f fluorescence in the majority of RP3V^{KISS1} neurons (Figures 1C, E). In slices obtained from male Kiss1-Cre::GCaMP6f mice, 5-HT-induced increases in fluorescence could also be observed (Figures 1D, F), but these responses were seen much less frequently (see below).

Because 5-HT signaling may be involved in the generation of the LH surge, we examined RP3V^{KISS1} neuron responses to 5-HT across the estrous cycle. As illustrated in Figure 2A, 5-HT-induced increases in RP3V^{KISS1} neuron fluorescence could be seen in slices from diestrous, proestrous and estrous mice and were larger than those seen in slices from male mice. The proportions of RP3V^{KISS1} neurons excited by 5-HT were similar at all cycle stages (diestrus: 85.3%, proestrus: 87.5%, estrus: 82.0%; $p > 0.18$, Fisher's exact tests) and were significantly higher than in males (29.1%; $p < 0.001$, Fisher's exact tests; Figure 2B and Table 1). The magnitude of RP3V^{KISS1} neuron responses to 5-HT significantly varied across these groups, with male responses significantly smaller than those in females at any estrous cycle stage, but no statistical differences across the estrous cycle (Table 1; Figure 2C). Smaller responses to 5-HT in males *versus* females could not be explained by a reduced ability of male RP3V^{KISS1} neurons to mount changes in $[Ca^{2+}]_i$, as responses to the glutamate receptor agonist AMPA were, in fact, larger in males than in females in those slices that were tested in this manner (Table 2).

Together, these observations indicate that RP3V^{KISS1} neuron responses to exogenous 5-HT are – to some extent – sex-dependent, being more prominent in females. Female responses, however, are not affected by the estrous cycle. The remainder of the study was conducted in brain slices from females.

3.2 5-HT increases female RP3V^{KISS1} neuron action potential firing

We then investigated if the effect of 5-HT was associated with changes in electrical activity in RP3V^{KISS1} neurons. In slices from female Kiss1-hrGFP mice, we recorded individual RP3V GFP-expressing neurons in the cell-attached configuration. Bath applications of 5-HT (one minute, 50 µM) increased action potential firing in just over half (52.9%) of RP3V^{KISS1} neurons (9 out of 17 neurons in 8 slices from 5 mice [1 di- and 4 estrus]; Figures 3A, C), decreased it in a few cells (2 cells [11.8% of total] in 2 slices from 2 mice [1 di- and 1 estrus]; Figures 3B, C), or did not affect firing (6 neurons [35.3% of total] in 5 slices from 4 mice [1 pro-, 1 di- and 2 estrus]). In those RP3V^{KISS1} neurons that were stimulated by 5-HT, action potential firing increased from 2.20 ± 0.42 to 6.33 ± 1.40 Hz ($p < 0.01$, $t = 3.66$, $df = 8$, paired t-test; Figure 3D). In the two cells inhibited by 5-HT, spontaneous firing (0.73 and 0.12 Hz) was transiently silenced in both cases.

These observations indicate that 5-HT primarily stimulates RP3V^{KISS1} neuron action potential firing. While 5-HT could also suppress firing in RP3V^{KISS1} neurons, this was seen much less frequently.

10.3389/fendo.2023.1212854

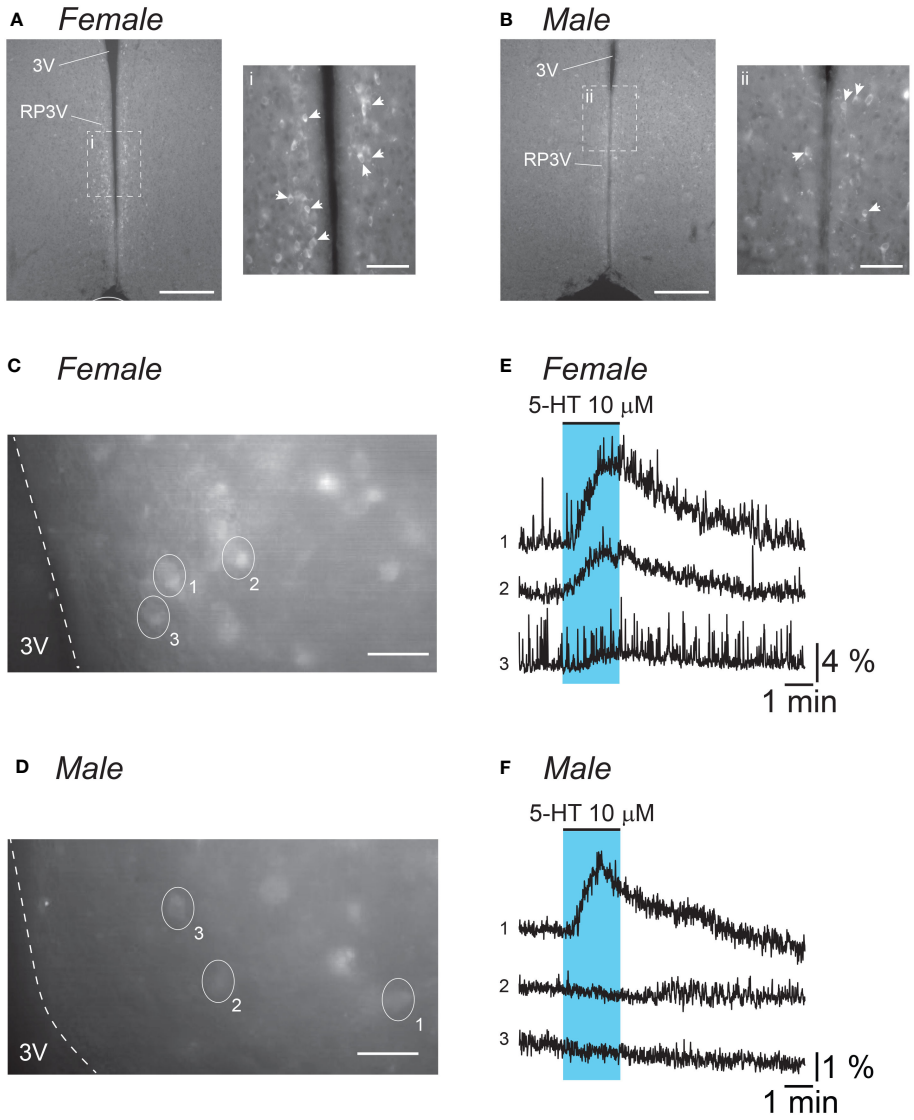

FIGURE 1
5-HT stimulates RP3V^{KISS1} neuron activity. **(A, B)** Low magnification (10X) epifluorescence images of endogenous GCaMP6f fluorescence in fixed coronal slices (30 µm thick) including the RP3V from a diestrous female **(A)** and a male **(B)** mouse. Insets i and ii are 20X magnification images of areas framed (dashed lines) in the low magnification images. Similar GCaMP6f-expressing cell distribution was observed in two different animals of each sex. White arrowheads indicate individual GCaMP6f-expressing neurons. 3V: third ventricle. Scale bars are 200 µm (50 µm in i and ii). **(C, D)** Epifluorescence images (40X magnification, average projection of 240 frames) of endogenous GCaMP6f fluorescence in acute coronal slices (200 µm thick) including the RP3V obtained from an estrous female **(C)** and a male **(D)** mouse. Ovals and numbers indicate individual regions of interest (ROIs) each including a single cell. Dashed lines delineate the border of the 3V. Scale bars 25 µm. **(E, F)** Normalized fluorescence traces for the ROIs delineated in C and D. Blue shading indicates the timing of 5-HT bath applications. Please note the difference in scale for normalized fluorescence in female **(E)** *versus* male traces **(F)**.

3.3 The effect of 5-HT on female RP3V^{KISS1} neuron $[Ca^{2+}]_i$ is direct

We next tested whether the effect of 5-HT is direct or mediated through the release of an intermediary factor by cells within the slice. To do this, we used a protocol in which slices from Kiss1-Cre:: GCaMP6f females were exposed to 5-HT (two minutes, 10 µM) twice at a 15- to 20-minute interval, the second 5-HT application being carried out in the presence of the voltage-gated sodium channel inhibitor tetrodotoxin (TTX; 0.5 µM) to block electrical activity in the slice. This concentration of TTX is sufficient to inhibit action potential generation in *ex vivo* preparations (57–59). As illustrated in Figure 4A, 5-HT-induced increases in RP3V^{KISS1} neuron fluorescence persisted in the presence of TTX. In control conditions, 57 out of 68 cells (83.8%) were stimulated by 5-HT. In the presence of TTX, 53 of these neurons (77.9% of the total; p = 0.51, Fisher's exact test; Figure 4B) displayed 5-HT-induced increases in normalized fluorescence. On average, 5-HT increased RP3V^{KISS1} neuron normalized fluorescence to a similar extent whether in the absence (2.72 ± 0.37%) or in the presence of TTX (2.34 ± 0.37%; n = 57 from 7 slices in 4 mice [2 pro-, 1 di- and 1 estrus]; p = 0.24, Wilcoxon test; Figure 4C).

10.3389/fendo.2023.1212854

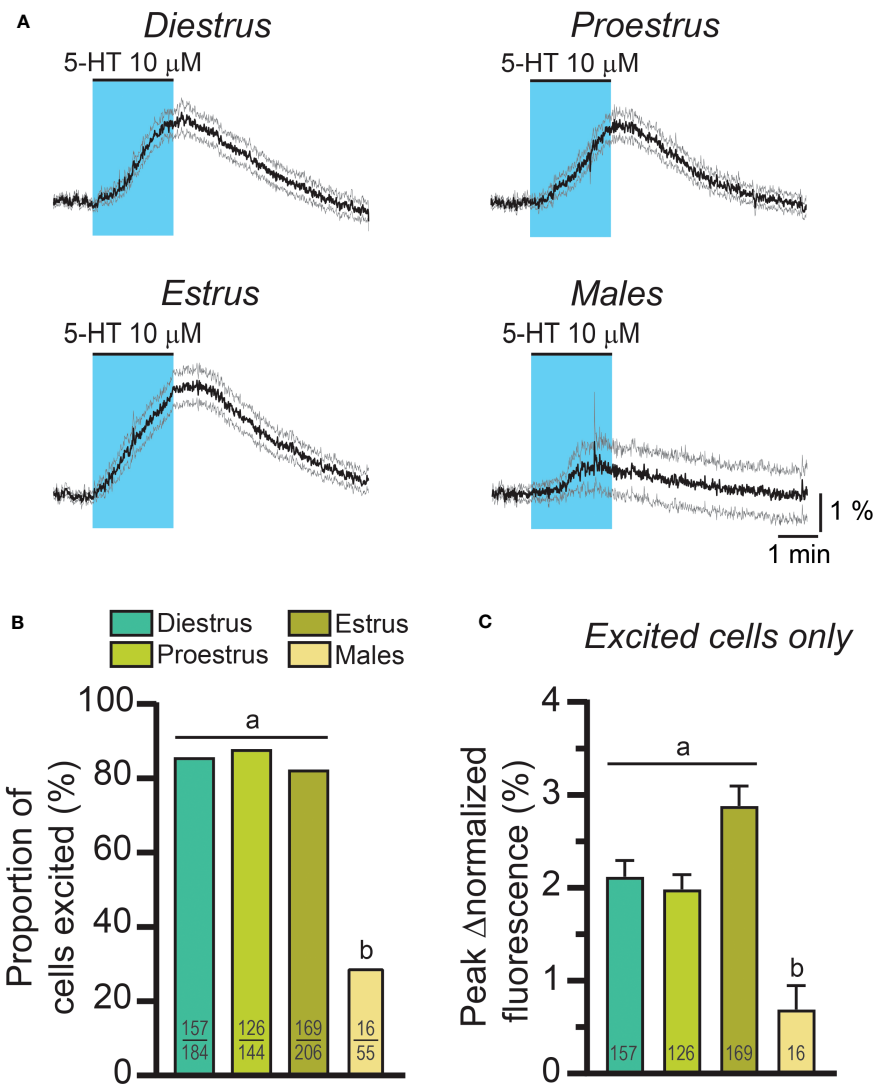

FIGURE 2
The effect of exogenous 5-HT on RP3V^{KISS1} neuron activity across the estrous cycle and in males. **(A)** 5-HT-induced changes in RP3V^{KISS1} neuron normalized fluorescence across the estrous cycle and in males. Traces are means (*black*) ± 95% confidence intervals (*grey*). **(B)** Similar proportions of RP3V^{KISS1} neurons were stimulated by 5-HT across the estrous cycle. This proportion was significantly lower in males. Numbers in bars are sample sizes (excited cells/total cells). **(C)** Peak 5-HT effect did not vary as a function of estrous cycle stage but was significantly smaller in males. Numbers in bars are sample sizes. Letters indicate results of statistical tests [Fisher's exact tests in **(B)** Kruskal-Wallis and Dunn's post-tests in **(C)**]. Bars with different letters are significantly different ($p < 0.05$; see Table 1 for details).

This finding indicates that the effect of 5-HT on RP3V^{KISS1} neuron activity is likely direct.

3.4 Activation of 5-HT$_2$ receptors mimics the effect of 5-HT in female RP3V^{KISS1} neurons

Because female RP3V^{KISS1} neurons express genes for multiple stimulatory 5-HT receptor subtypes, including *htr2a*, *htr2c*, *htr3a*, *htr4*, *htr6* and *htr7* (60), we next examined if activating these 5-HT receptors could increase $[Ca^{2+}]_i$ in female RP3V^{KISS1} neurons. Increases in RP3V^{KISS1} neuron activity could be seen in response to bath-applications of the agonists TCB-2 (1 μM; 5-HT$_{2A}$ receptors; 2 di-, 1 pro- and 1 estrous mice), WAY161503 (10 μM; 5-HT$_{2C}$ receptors; 3 diestrous mice), SR57227 (1 μM; 5-HT$_3$ receptors; 4 diestrous mice), cisapride (1 μM; 5-HT$_4$ receptors; 3 diestrous mice), WAY208466 (10 μM; 5-HT$_6$ receptors; 3 diestrous mice) and AS19 (10 μM; 5-HT$_7$ receptors; 1 di-, 3 pro- and 1 estrous mice) (Figures 5A, B and Table 3). However, activating 5-HT$_{2A}$ and 5-HT$_{2C}$ receptors resulted in greater proportions of stimulated RP3V^{KISS1} neurons (≈55-70%) than activating other receptor subtypes (Figure 5C and Table 3). In addition, activating 5-HT$_{2C}$ receptors resulted in significantly larger responses than activating other 5-HT receptors, whereas responses to 5-HT$_{2A}$ receptor activation were rather moderate in magnitude (Figure 5D and Table 3).

Taken together, these observations indicate that the female RP3V^{KISS1} neuron population expresses multiple functional excitatory 5-HT receptor subtypes. However, of these, activation

10.3389/fendo.2023.1212854

TABLE 1 RP3V^{KISS1} neuron responses to 5-HT across the female estrous cycle and in males.

	Diestrus	Proestrus	Estrus	Male
Total cell number	184	144	206	55
Excited cell number (proportion)	157 (85.3%)	126 (87.5%)	169 (82.0%)	16 (29.1%)
Fisher's exact tests	p = 0.63 *versus* proestrus	p = 0.18 *versus* estrus	p = 0.41 *versus* diestrus	p < 0.001 *versus* diestrus, proestrus and estrus
Peak Δnormalized fluorescence (excited cells only)	2.12 ± 0.17%	1.98 ± 0.16%	2.88 ± 0.21%	0.69 ± 0.26%
Kruskal-Wallis test[a]	p < 0.001, K-S statistic = 22.37			
Dunn's post-tests	p > 0.99 *versus* proestrus	p = 0.20 proestrus *versus* estrus	p = 0.12 *versus* diestrus	p < 0.001 *versus* diestrus and proestrus p < 0.001 *versus* estrus
Slice (mouse) number	14 (10)	12 (11)	17 (10)	6 (5)[b]

[a]the Kruskal-Wallis test was used to test for statistical differences across all 4 groups (males, di-, pro- and estrous females).
[b]the 16 male neurons that responded were in 4 slices from 3 different males.

of 5-HT$_2$ receptors, in particular 5-HT$_{2C}$, most closely mimics the effect of 5-HT on female RP3V^{KISS1} neurons.

3.5 5-HT stimulates female RP3V^{KISS1} neuron activity *via* activation of 5-HT$_2$ receptors

Based on these findings, we then sought to determine the role of 5-HT$_2$ receptors in mediating the effect of 5-HT on RP3V^{KISS1} neuron activity. Using a dual 5-HT application protocol like that described above, we tested the impact of 5-HT$_2$ receptor antagonists on RP3V^{KISS1} neuron responses to 5-HT. As illustrated in Figure 6A, the antagonist ritanserin (5 μM), which prevents the LH surge in rats (34), almost completely blocked the effect of 5-HT in RP3V^{KISS1} neurons. 69 out of 85 cells (81.2%) were stimulated by 5-HT in control conditions. In the presence of ritanserin, 31 of these (36.5% of the total; p < 0.001, Fisher's exact test) had 5-HT-induced increases in normalized fluorescence (Figure 6B). On average, 5-HT-induced changes in RP3V^{KISS1} neuron normalized fluorescence were substantially reduced by ritanserin (0.29 ± 0.10% *versus* 3.37 ± 0.32% in the absence of antagonist; n = 69 in 5 slices from 5 mice [2 pro-, 2 di- and 1 estrus]; p < 0.001, sum of signed ranks (W) = -2387, Wilcoxon test; Figure 6C). The same held true when only those cells that were excited by 5-HT in the presence of ritanserin were considered (Table 4). Similar results were obtained with the antagonist mianserin (10 μM). In its presence, only 8 out of 75 cells (10.7% *versus* 80.0% [60 out of 75] in control; p < 0.001, Fisher's exact test; Figure 6D) were excited by 5-HT. Moreover, 5-HT-induced increases in normalized fluorescence were significantly suppressed by mianserin (-0.53 ± 0.22% *versus* 2.61 ± 0.42% in the absence of antagonist; n = 60 in 6 slices from 5 mice [1 pro-, 2 di- and 2 estrus]; p < 0.001, sum of signed ranks (W) = -1718, Wilcoxon test; Figure 6E), even when only cells stimulated by 5-HT in the presence of the antagonist were considered (Table 4).

Together with the results obtained using 5-HT receptor agonists, these data indicate that the effect of 5-HT on RP3V^{KISS1} neurons is – for the most part – mediated by 5-HT$_2$ receptors, likely through the combined effect of 5-HT$_{2A}$ and 5-HT$_{2C}$ receptor activation.

4 Discussion

We report here using GCaMP-based $[Ca^{2+}]_i$ imaging and electrophysiology that exogenous 5-HT stimulates the activity of a majority of RP3V^{KISS1} neurons in female mice. This effect is observed in higher proportions of RP3V^{KISS1} neurons – and with larger magnitudes – in females than in males. In females, however, the effect of 5-HT does not significantly vary between estrous cycle stages. Lastly, we find that 5-HT-induced excitations are likely mediated directly at RP3V^{KISS1} neurons and that these effects require activation of 5-HT$_2$ receptors. Together, these observations suggest that stimulation of RP3V^{KISS1} neurons might be a mechanism through which 5-HT influences the LH surge in rodents.

A large proportion of female RP3V^{KISS1} neurons (> 80%) exhibited increases in $[Ca^{2+}]_i$ in response to 5-HT in brain slices

TABLE 2 Response of female and male RP3V^{KISS1} neurons to stimulation by AMPA.

	Female	Male
Total cell number	299[a]	16[a]
Peak Δnormalized fluorescence (excited cells only)	18.75 ± 0.85%	27.49 ± 3.70%
Mann-Whitney test	p = 0.01, Mann-Whitney U = 1496	
Slice (mouse) number	27 (20)	4 (3)

[a]includes only those cells that responded to 5-HT.

10.3389/fendo.2023.1212854

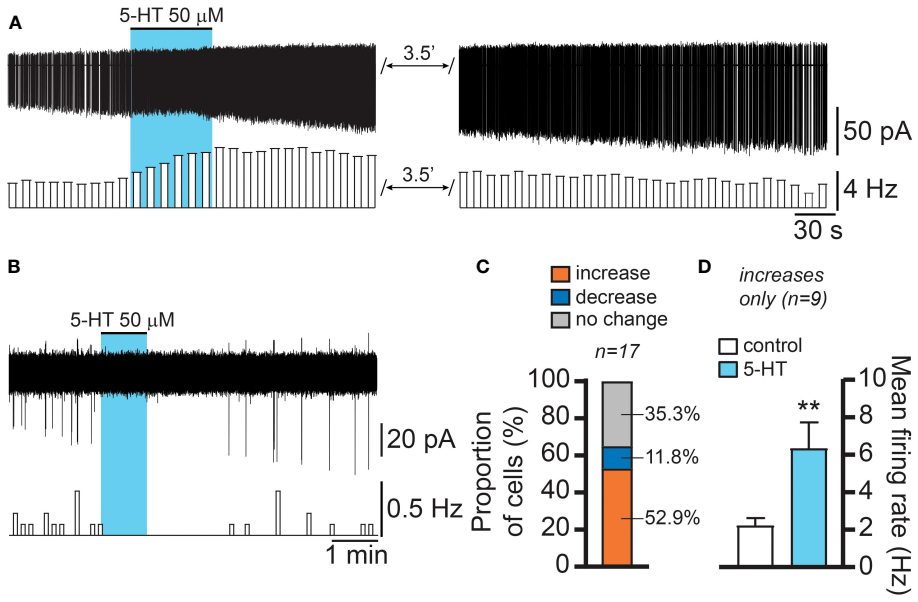

FIGURE 3
5-HT effects on female RP3V^{KISS1} neuron action potential firing. **(A, B)** Example traces and corresponding rate-meters illustrating the excitatory **(A)** and inhibitory **(B)** effects of 5-HT on female RP3V^{KISS1} neuron firing. Blue shading indicates the timing of 5-HT bath applications. **(C)** Proportions of RP3V^{KISS1} neurons that showed increased, decreased or no change in firing in response to 5-HT. **(D)** In those cells that were excited by 5-HT, the increase in firing was statistically significant. **p < 0.01 paired t-test. Numbers above bars are sample sizes.

from Kiss1-Cre::GCaMP6f mice. In slices from Kiss1-hrGFP mice, 5-HT caused an increase in action potential firing in > 50% of RP3V^{KISS1} neurons. Increases in $[Ca^{2+}]_i$ induced by 5-HT likely result from opening of voltage-gated Ca^{2+} channels in response to action potential firing and/or to subthreshold membrane depolarization, from G-protein-dependent Ca^{2+} release from internal stores, or from a combination thereof (10, 61). As the cell-attached patch-clamp recording configuration does not give access to subthreshold membrane potential fluctuations – nor to changes in $[Ca^{2+}]_i$ – the proportions of neurons that responded to 5-HT applications with elevations in $[Ca^{2+}]_i$ and in firing rates cannot be directly compared. Interestingly, 5-HT suppressed firing in a small subset (≈ 10%) of RP3V^{KISS1} neurons in electrophysiology experiments. It is possible that such responses were not seen with our $[Ca^{2+}]_i$ imaging because, at least under our recording conditions, this approach does not effectively resolve inhibitions in those cells that display low resting activity levels (10, 61). Nevertheless, our observation that 5-HT stimulated activity in a majority of RP3V^{KISS1} neurons is in line with a recent report that 5-HT increases firing in arcuate kisspeptin (ARC^{KISS1}) neurons (62), suggesting that stimulation by 5-HT is a common feature of hypothalamic kisspeptin neurons. Somewhat contrastingly, only a small proportion of adult female GnRH neurons (< 40%) are stimulated by 5-HT, whereas most (≈ 75%) are inhibited (46).

The stimulatory effect of 5-HT on RP3V^{KISS1} neuron $[Ca^{2+}]_i$ was largely resistant to blockade of action potential firing, suggesting that responses to 5-HT were mediated primarily through action potential-independent VGCC opening and/or

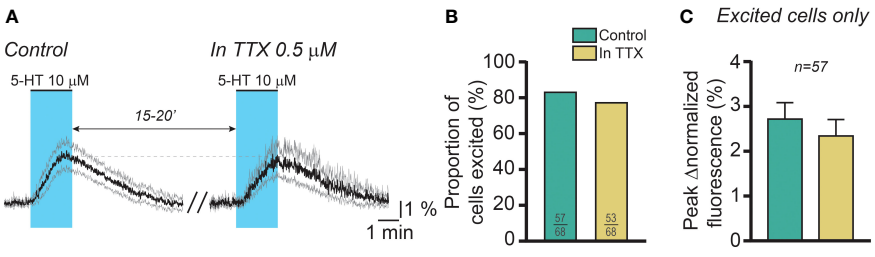

FIGURE 4
The effect of 5-HT on female RP3V^{KISS1} neuron activity is direct. **(A)** 5-HT was applied twice to brain slices from female mice, at 15-to-20-minute intervals. The first application (control; *left*) was carried out in the absence of drugs whereas the second was conducted in the continuous presence of tetrodotoxin (TTX; *right*) to block action potentials. Traces are means (*black*) ± 95% confidence intervals (*grey*) and include those RP3V^{KISS1} neurons that were stimulated by 5-HT upon the first application (n = 57). Blue shading indicates the timing of 5-HT bath applications. **(B)** Similar proportions of RP3V^{KISS1} neurons were stimulated by 5-HT in the presence and in the absence of TTX. Numbers in bars are sample sizes (excited cells/total cells). **(C)** The peak magnitude of the 5-HT effect was similar in the presence and in the absence of TTX. Only RP3V^{KISS1} neurons excited by 5-HT upon the first application were included in this analysis. The number above the bars is the sample size.

10.3389/fendo.2023.1212854

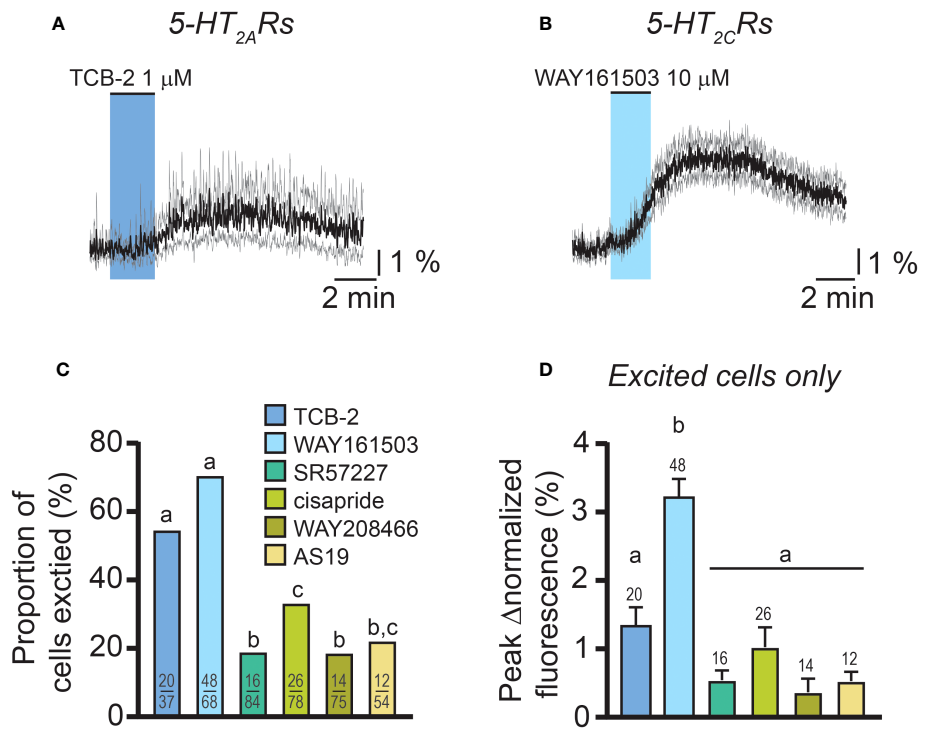

FIGURE 5
Responses of female RP3V^{KISS1} neurons to excitatory 5-HT receptor agonists. **(A, B)** Average responses of female RP3V^{KISS1} neurons stimulated by 5-HT_{2A} **(A)** and 5-HT_{2C} **(B)** receptor agonists. Colored shading indicates the timing of agonist applications. Traces are means (*black*) ± 95% confidence intervals (*grey*). **(C)** Proportions of female RP3V^{KISS1} neurons stimulated by 5-HT receptor agonists. Numbers in bars are sample sizes (excited cells/total cells). **(D)** Magnitude of the effect of different 5-HT receptor agonists. Only RP3V^{KISS1} neurons that responded to agonists were included in this analysis. Numbers above bars are sample sizes. Letters above bars represent the results of statistical tests [Fisher's exact tests in **(C)** and Kruskal-Wallis and Dunn's post-tests in **(D)**]. Bars that do not share a letter are significantly different ($p < 0.05$, see Table 3 for details).

mobilization of intracellular Ca^{2+} stores. This also reveals that RP3V^{KISS1} neuron $[Ca^{2+}]_i$ responses to 5-HT were independent on electrical activity within the brain slice and, therefore, resulted from direct 5-HT actions at the kisspeptin neurons. Moreover, RP3V^{KISS1} neurons displayed excitatory responses to 5-HT_{2A}, 5-HT_{2C}, 5-HT_3, 5-HT_4, 5-HT_6 and 5-HT_7 receptor activation. This reveals that RP3V^{KISS1} neurons may express multiple functional 5-HT receptor subtypes. However, activation of 5-HT_{2C} and – to a lesser extent – 5-HT_{2A} receptors most closely mimicked the stimulatory effect of 5-HT. Importantly, the stimulatory effect of 5-HT was blocked by the 5-HT_2 receptor antagonists ritanserin and mianserin. Together, these observations indicate that 5-HT

TABLE 3 RP3V^{KISS1} neuron excitatory responses to 5-HT receptor agonists in female mice.

	TCB-2	WAY161503	SR57227	Cisapride	WAY208466	AS19
Total cell number	37	68	84	78	75	54
Excited cell number (proportion)	20 (54.1%)	48 (70.6%)	16 (19.0%)	26 (33.3%)	14 (18.7%)	12 (22.2%)
Fisher's exact tests	$p < 0.001$ *versus* SR57227 and WAY208466	$p < 0.001$ *versus* SR57227, cisapride, WAY208466 and AS19	$p < 0.05$ *versus* cisapride	$p < 0.05$ *versus* TCB-2	$p < 0.05$ *versus* cisapride	$p < 0.01$ *versus* TCB-2
Peak Δnormalized fluorescence (excited cells only)	1.33 ± 0.28%	3.21 ± 0.28%	0.54 ± 0.14%	1.03 ± 0.29%	0.37 ± 0.20%	0.53 ± 0.14%
Kruskal-Wallis test[a]	$p < 0.001$, K-S statistic = 62.09					
Dunn's post-tests	/	$p < 0.01$ *versus* TCB-2	$p < 0.001$ *versus* WAY161503	$p < 0.001$ *versus* WAY161503	$p < 0.001$ *versus* WAY161503	$p < 0.001$ *versus* WAY161503
Slice (mouse) number	5 (4)	5(3)	7 (4)[b]	6(3)	5(3)[b]	5(5)[b]

[a]the Kruskal-Wallis test was used to test for statistical differences across the effect of all 6 agonists (TCB-2, WAY161503, SR57227, cisapride, WAY208466 and AS19).
[b]RP3V^{KISS1} cells showing excitatory responses to SR57227, WAY208466 and to AS19 were found in 6 slices from 4 mice, in 4 slices from 3 mice and in 3 slices from 3 mice, respectively.

10.3389/fendo.2023.1212854

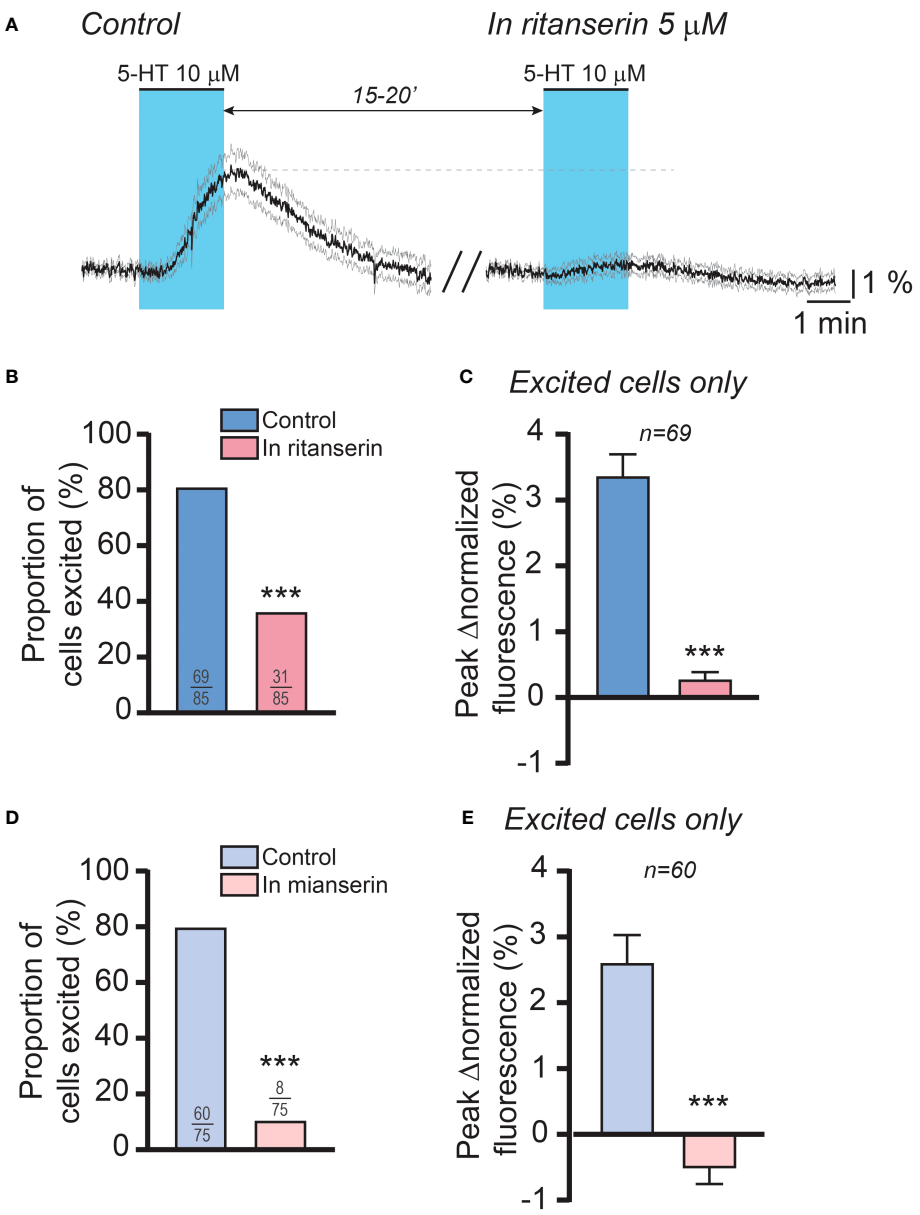

FIGURE 6
5-HT2 receptors mediate the effect of 5-HT on female RP3V^{KISS1} neuron activity. **(A)** 5-HT was applied twice to female brain slices, at 15-to-20-minute intervals. The first application (control; *left*) was carried out in the absence of drugs whereas the second was conducted in the continuous presence of ritanserin (*right*), a 5-HT2 receptor antagonist. Light blue shading indicates the timing of 5-HT bath applications. Traces are means (*black*) ± 95% confidence intervals (*grey*). **(B)** Proportions of RP3V^{KISS1} neurons stimulated by 5-HT significantly decreased in the presence of ritanserin. ***p < 0.001, Fisher's exact test. Numbers in bars are sample sizes (excited cells/total cells). **(C)** Ritanserin significantly decreased the peak magnitude of the 5-HT effect. ***p < 0.001, Wilcoxon signed rank test. Number above bars is the sample size. **(D)** Mianserin significantly reduced the proportions of RP3V^{KISS1} neurons stimulated by 5-HT. ***p < 0.001, Fisher's exact test. Numbers in bars are sample sizes (excited cells/total cells). **(E)** The peak magnitude of the 5-HT effect was significantly suppressed by mianserin. ***p < 0.001, Wilcoxon signed rank test. Number above bars is the sample size. Only RP3V^{KISS1} neurons that responded to 5-HT upon the first bath application were included in the analyses displayed in **(C, E)**.

TABLE 4 Excitatory effects of 5-HT in the presence of 5-HT$_2$ receptor antagonists ritanserin or mianserin.

	Control (Peak Δnormalized fluorescence)	In antagonist (Peak Δnormalized fluorescence)	number of cells (slices; mice)	Wilcoxon signed rank tests
Ritanserin	2.99 ± 0.38%	0.55 ± 0.10%	31 (3; 3[a])	p < 0.001, sum of signed ranks W = -490
Mianserin	5.31 ± 1.62%	0.03 ± 0.66%	8 (5; 4[a])	p < 0.05, sum of signed ranks W = -32

[a]ritanserin: 2 pro- and 1 estrous mice; mianserin: 1 pro-, 1 di- and 2 estrous mice.

stimulates RP3V^{KISS1} neuron activity by acting at 5-HT$_2$ receptors, including 5-HT$_{2A}$ and 5-HT$_{2C}$ receptors. 5-HT is also reported to stimulate the activity of ARC^{KISS1} neurons, but this is mostly mediated by 5-HT$_4$ receptors (62). The two main populations of hypothalamic kisspeptin neurons may, therefore, have different functional 5-HT receptor make-ups. Nevertheless, our observations in RP3V^{KISS1} neurons are in line with previous reports that ritanserin prevents the LH surge in rats (33, 34), and that activation of 5-HT$_{2A}$ and 5-HT$_{2C}$ receptors restores the LH surge in DR-lesioned female rats (26). Seeing the pattern and pharmacology of RP3V^{KISS1} neuron responses to 5-HT – and, as discussed above, that 5-HT may primarily inhibit female GnRH neurons (46) – we propose that the stimulatory effect of 5-HT we report here might be involved in mediating the previously reported excitatory influence of 5-HT neurotransmission on the LH surge (27–30, 32–34).

5-HT responses were found in a substantially and significantly lower proportion of RP3V^{KISS1} neurons in males (≈ 35%) than in females. Further, those male RP3V^{KISS1} neurons that were stimulated by 5-HT displayed much smaller responses than their female counterparts. Although we cannot fully rule out that a proportion of the GCaMP6f-expressing cells that we recorded in slices from male mice were RP3V neurons that do not, in fact, express *Kiss1* (10, 63–65), this suggests that 5-HT excitatory effects in RP3V^{KISS1} neurons display some degree of sex-dependence. As the LH surge mechanism, including many aspects of the RP3V^{KISS1} → GnRH neural circuit, is sexually differentiated in rodents (66–69), this observation suggests that 5-HT signaling in RP3V^{KISS1} neurons might be part of the mechanism activating these cells for the surge. On the other hand, we find that the impact of 5-HT on RP3V^{KISS1} neuron activity did not significantly change between estrous cycle stages, with similar proportions of neurons stimulated and similar response magnitude. This suggests that regulation of 5-HT$_2$ receptor function in RP3V^{KISS1} neurons might not be a mechanism through which these cells are specifically activated for the proestrous surge. Rather, this suggests that 5-HT might have a permissive effect on RP3V^{KISS1} neuron activity as it does on the surge *in vivo* (15). On the other hand, 5-HT content and turnover in the hypothalamus, including the POA, might fluctuate around the time of the proestrous surge in a diurnal manner (28, 70, 71). Whether 5-HT release in the vicinity of RP3V^{KISS1} neurons fluctuates in a time- and estrous cycle-dependent manner is unknown but would be anticipated to affect RP3V^{KISS1} neuron activity.

5-HT-containing fibers are detected within the RP3V in male and female rats (38–40), but it is unknown whether these fibers are in the vicinity of kisspeptin neurons. The origin of these fibers is also unknown. They may originate in the DR as lesions of this area, more so than lesions of the medial raphe nucleus, prevent the LH surge (23–26). Curiously, electrical stimulation of the DR fails at altering the LH surge in proestrous rats (24), whereas this manipulation can evoke LH secretion in E-replaced OVX rats (72) and result in a subtle prolongation of LH secretion evoked by stimulation of the POA (73). DR neurons project directly to POA GnRH neurons (42); whether they project to RP3V^{KISS1} neurons will need to be established by tract-tracing experiments. It should be noted that 5-HT transporter-immunoreactive fibers are seen in close apposition to ARC^{KISS1} neurons (62). As ARC^{KISS1} neurons might be involved in regulating the LH surge (74–78), it is possible that these fibers contribute to the influence of 5-HT on the surge. As discussed above, the pharmacology of ARC^{KISS1} neuron responses to 5-HT does not match that of the influence of 5-HT on the surge, however.

Lastly, the type of information that 5-HT neurons relay to the GnRH neuronal network to regulate the surge is unknown. 5-HT may mediate the permissive effect of the metabolic hormone leptin on the hypothalamic-pituitary-gonadal axis (79) and, indeed, the DR is involved in many aspects of energy balance (80). Additionally, 5-HT signaling may be involved in regulating circadian rhythms and responses to stressors (81–83), which also affect LH secretion and the surge (20, 21). Further studies will be required to determine the precise contribution of changes in 5-HT neurotransmission in regulating the surge and whether this involves RP3V^{KISS1} neurons.

In conclusion, the findings reported here regarding the stimulatory effect of 5-HT signaling on RP3V^{KISS1} neuron activity contribute to our understanding of the brain circuits that control ovulation in females.

Data availability statement

The raw data supporting the conclusions of this article will be made available by the authors, without undue reservation.

Ethics statement

The animal study was approved by Kent State University Institutional Animal Care and Use Committee. The study was conducted in accordance with the local legislation and institutional requirements.

Author contributions

RP designed the research. CB, RB, AN, AA and JD carried out the experiments. CB, RB, AN, AA, and RP analyzed the data. RP wrote the manuscript. All authors contributed to the article and approved the submitted version.

Funding

This work was supported by NICHD grant R01HD109337 to RP. Publication of this study was supported by the Department of Biological Sciences and the Open Access Publishing Fund at Kent State University.

Acknowledgments

We thank Drs. Bradley Jamieson and Aleisha Moore as well as members of the Piet laboratory for their comments on an earlier draft of this manuscript, Conor McDevitt for technical assistance

and Dr. Aleisha Moore for helping with taking pictures of GCaMP6f endogenous fluorescence in fixed tissue.

Conflict of interest

The authors declare that the research was conducted in the absence of any commercial or financial relationships that could be construed as a potential conflict of interest.

Publisher's note

References

1. Goodman RL, Herbison AE, Lehman MN, Navarro VM. Neuroendocrine control of gonadotropin-releasing hormone: pulsatile and surge modes of secretion. *J Neuroendocrinol* (2022) 34(5):e13094. doi: 10.1111/jne.13094

2. Herbison AE, Robinson JE, Skinner DC. Distribution of estrogen receptor-immunoreactive cells in the preoptic area of the ewe: co-localization with glutamic acid decarboxylase but not luteinizing hormone-releasing hormone. *Neuroendocrinology* (1993) 57(4):751–9. doi: 10.1159/000126433

3. Herbison AE, Theodosis DT. Localization of oestrogen receptors in preoptic neurons containing neurotensin but not tyrosine hydroxylase, cholecystokinin or luteinizing hormone-releasing hormone in the male and female rat. *Neuroscience* (1992) 50(2):283–98. doi: 10.1016/0306-4522(92)90423-y

4. Lehman MN, Ebling FJ, Moenter SM, Karsch FJ. Distribution of estrogen receptor-immunoreactive cells in the sheep brain. *Endocrinology* (1993) 133(2):876–86. doi: 10.1210/endo.133.2.8344223

5. Wintermantel TM, Campbell RE, Porteous R, Bock D, Grone HJ, Todman MG, et al. Definition of estrogen receptor pathway critical for estrogen positive feedback to gonadotropin-releasing hormone neurons and fertility. *Neuron* (2006) 52(2):271–80. doi: 10.1016/j.neuron.2006.07.023

6. Glidewell-Kenney C, Hurley LA, Pfaff L, Weiss J, Levine JE, Jameson JL. Nonclassical estrogen receptor alpha signaling mediates negative feedback in the female mouse reproductive axis. *Proc Natl Acad Sci U.S.A.* (2007) 104(19):8173–7. doi: 10.1073/pnas.0611514104

7. Herbison AE. Physiology of the Adult Gonadotropin-Releasing Hormone Neuronal Network. In: Plant TM, Zeleznik AJ, editors. *Knobil and Neill's Physiology of Reproduction*. San Diego: Academic Press (2015). p. 399–467.

8. Clarkson J, Herbison AE. Oestrogen, kisspeptin, gpr54 and the pre-ovulatory luteinising hormone surge. *J Neuroendocrinol* (2009) 21(4):305–11. doi: 10.1111/j.1365-2826.2009.01835.x

9. Herbison AE. Estrogen positive feedback to gonadotropin-releasing hormone (Gnrh) neurons in the rodent: the case for the rostral periventricular area of the third ventricle (Rp3v). *Brain Res Rev* (2008) 57(2):277–87. doi: 10.1016/j.brainresrev.2007.05.006

10. Jamieson BB, Piet R. Kisspeptin neuron electrophysiology: intrinsic properties, hormonal modulation, and regulation of homeostatic circuits. *Front Neuroendocrinol* (2022) 66:101006. doi: 10.1016/j.yfrne.2022.101006

11. Kauffman AS. Neuroendocrine mechanisms underlying estrogen positive feedback and the lh surge. *Front Neurosci* (2022) 16:953252. doi: 10.3389/fnins.2022.953252

12. Starrett JR, Moenter SM. Hypothalamic kisspeptin neurons as potential mediators of estradiol negative and positive feedback. *Peptides* (2023) 163:170963. doi: 10.1016/j.peptides.2023.170963

13. Kordon C, Glowinski J. Role of hypothalamic monoaminergic neurones in the gonadotrophin release-regulating mechanisms. *Neuropharmacology* (1972) 11(2):153–62. doi: 10.1016/0028-3908(72)90088-3

14. Kalra SP, Kalra PS. Neural regulation of luteinizing hormone secretion in the rat. *Endocr Rev* (1983) 4(4):311–51. doi: 10.1210/edrv-4-4-311

15. Vitale ML, Chiocchio SR. Serotonin, a neurotransmitter involved in the regulation of luteinizing hormone release. *Endocr Rev* (1993) 14(4):480–93. doi: 10.1210/edrv-14-4-480

16. Herbison AE. Noradrenergic regulation of cyclic gnrh secretion. *Rev Reprod* (1997) 2(1):1–6. doi: 10.1530/ror.0.0020001

17. Spergel DJ. Modulation of gonadotropin-releasing hormone neuron activity and secretion in mice by non-peptide neurotransmitters, gasotransmitters, and gliotransmitters. *Front Endocrinol (Lausanne)* (2019) 10:329. doi: 10.3389/fendo.2019.00329

18. Spergel DJ. Neuropeptidergic modulation of gnrh neuronal activity and gnrh secretion controlling reproduction: insights from recent mouse studies. *Cell Tissue Res* (2019) 375(1):179–91. doi: 10.1007/s00441-018-2893-z

19. Navarro VM. Metabolic regulation of kisspeptin - the link between energy balance and reproduction. *Nat Rev Endocrinol* (2020) 16(8):407–20. doi: 10.1038/s41574-020-0363-7

20. McCosh RB, O'Bryne KT, Karsch FJ, Breen KM. Regulation of the gonadotropin-releasing hormone neuron during stress. *J Neuroendocrinol* (2022) 34(5):e13098. doi: 10.1111/jne.13098

21. Piet R. Circadian and kisspeptin regulation of the preovulatory surge. *Peptides* (2023) 163:170981. doi: 10.1016/j.peptides.2023.170981

22. Iremonger KJ, Constantin S, Liu X, Herbison AE. Glutamate regulation of gnrh neuron excitability. *Brain Res* (2010) 1364(10 December 2010):35–43. doi: 10.1016/j.brainres.2010.08.071

23. Hery M, Laplante E. Kordon C. Participation of serotonin in the phasic release of luteinizing hormone. Ii. Effects of lesions of serotonin-containing pathways in the central nervous system. *Endocrinology* (1978) 102(4):1019–25. doi: 10.1210/endo-102-4-1019

24. Morello H, Taleisnik S. Changes of the release of luteinizing hormone (Lh) on the day of proestrus after lesions or stimulation of the raphe nuclei in rats. *Brain Res* (1985) 360(1-2):311–7. doi: 10.1016/0006-8993(85)91247-8

25. Vitale ML, Villar MJ, Chiocchio SR, Tramezzani JH. Dorsal raphe lesion alters the estrous cycle and the preovulatory gonadotropin release. *Neuroendocrinology* (1987) 46(3):252–7. doi: 10.1159/000124828

26. Maekawa F, Tsukahara S, Tsukamura H, Maeda KI, Yamanouchi K. Prevention of inhibitory effect of dorsal raphe nucleus lesions on ovulation and lh surge by 5-ht 2a/2c receptor agonists in female rats. *Neurosci Res* (1999) 35(4):291–8. doi: 10.1016/s0168-0102(99)00090-5

27. Hery M, Laplante E. Kordon C. Participation of serotonin in the phasic release of lh. I. Evidence from pharmacological experiments. *Endocrinology* (1976) 99(2):496–503. doi: 10.1210/endo-99-2-496

28. Walker RF. Serotonin neuroleptics change patterns of preovulatory secretion of luteinizing hormone in rats. *Life Sci* (1980) 27(12):1063–8. doi: 10.1016/0024-3205(80)90030-2

29. Horn AM, Fink G. Parachlorophenylalanine blocks the spontaneous pro-oestrous surge of prolactin as well as lh and affects the secretion of oestradiol-17 beta. *J Endocrinol* (1985) 104(3):415–8. doi: 10.1677/joe.0.1040415

30. Meyer DC, Eadens DJ. The role of endogenous serotonin in phasic lh release. *Brain Res Bull* (1985) 15(3):283–6. doi: 10.1016/0361-9230(85)90152-2

31. Burri R, Petersen SL, Barraclough CA. Effects of P-chlorophenylalanine on hypothalamic indoleamine levels and the associated changes which occur in catecholamine dynamics and lh surges in estrogen-treated ovariectomized rats. *Brain Res* (1987) 416(2):267–76. doi: 10.1016/0006-8993(87)90906-1

32. Tanaka E, Baba N, Toshida K, Suzuki K. Evidence for 5-ht2 receptor involvement in the stimulation of preovulatory lh and prolactin release and ovulation in normal cycling rats. *Life Sci* (1993) 52(7):669–76. doi: 10.1016/0024-3205(93)90459-g

33. Dow RC, Williams BC, Bennie J, Carroll S, Fink G. A central 5-ht2 receptor mechanism plays a key role in the proestrous surge of luteinizing hormone in the rat. *Psychoneuroendocrinology* (1994) 19(4):395–9. doi: 10.1016/0306-4530(94)90019-1

34. Fink G, Dow RC, McQueen JK, Bennie JG, Carroll SM. Serotonergic 5-ht2a receptors important for the oestradiol-induced surge of luteinising hormone-releasing hormone in the rat. *J Neuroendocrinol* (1999) 11(1):63–9. doi: 10.1046/j.1365-2826.1999.00299.x

35. Morello H, Taleisnik S. The inhibition of proestrous lh surge and ovulation in rats bearing lesions of the dorsal raphe nucleus is mediated by the locus coeruleus. *Brain Res* (1988) 440(2):227–31. doi: 10.1016/0006-8993(88)90990-0

36. Morello H, Caligaris L, Haymal B, Taleisnik S. Inhibition of proestrous lh surge and ovulation in rats evoked by stimulation of the medial raphe nucleus involves a gaba-mediated mechanism. *Neuroendocrinology* (1989) 50(1):81–7. doi: 10.1159/000125205

37. Morello H, Caligaris L, Haymal B, Taleisnik S. The pineal gland mediates the inhibition of proestrous luteinizing hormone surge and ovulation in rats resulting from stimulation of the medial raphe nucleus or injection of 5-ht into the third ventricle. *J Neuroendocrinol* (1989) 1(3):195–7. doi: 10.1111/j.1365-2826.1989.tb00102.x

38. Simerly RB, Swanson LW. The distribution of neurotransmitter-specific cells and fibers in the anteroventral periventricular nucleus: implications for the control of gonadotropin secretion in the rat. *Brain Res* (1987) 400(1):11–34. doi: 10.1016/0006-8993(87)90649-4

39. Simerly RB, Swanson LW, Gorski RA. The distribution of monoaminergic cells and fibers in a periventricular preoptic nucleus involved in the control of gonadotropin release: immunohistochemical evidence for a dopaminergic sexual dimorphism. *Brain Res* (1985) 330(1):55–64. doi: 10.1016/0006-8993(85)90007-1

40. Awasthi JR, Tamada K, Overton ETN, Takumi T. Comprehensive topographical map of the serotonergic fibers in the male mouse brain. *J Comp Neurol* (2021) 529 (7):1391–429. doi: 10.1002/cne.25027

41. Kiss J, Halasz B. Demonstration of serotoninergic axons terminating on luteinizing hormone-releasing hormone neurons in the preoptic area of the rat using a combination of immunocytochemistry and high resolution autoradiography. *Neuroscience* (1985) 14(1):69–78. doi: 10.1016/0306-4522(85)90164-2

42. Campbell RE, Herbison AE. Definition of brainstem afferents to gonadotropin-releasing hormone neurons in the mouse using conditional viral tract tracing. *Endocrinology* (2007) 148(12):5884–90. doi: 10.1210/en.2007-0854

43. Johnson MD, Crowley WR. Role of central serotonin systems in the stimulatory effects of ovarian hormones and naloxone on luteinizing hormone release in female rats. *Endocrinology* (1986) 118(3):1180–6. doi: 10.1210/endo-118-3-1180

44. Hery M, Francois-Bellan AM, Hery F, Deprez P, Becquet D. Serotonin directly stimulates luteinizing hormone-releasing hormone release from gt1 cells *via* 5-ht7 receptors. *Endocrine* (1997) 7(2):261–5. doi: 10.1007/BF02778149

45. Wada K, Hu L, Mores N, Navarro CE, Fuda H, Krsmanovic LZ, et al. Serotonin (5-ht) receptor subtypes mediate specific modes of 5-ht-induced signaling and regulation of neurosecretion in gonadotropin-releasing hormone neurons. *Mol Endocrinol* (2006) 20(1):125–35. doi: 10.1210/me.2005-0109

46. Bhattarai JP, Roa J, Herbison AE, Han SK. Serotonin acts through 5-ht1 and 5-ht2 receptors to exert biphasic actions on gnrh neuron excitability in the mouse. *Endocrinology* (2014) 155(2):513–24. doi: 10.1210/en.2013-1692

47. Chen TW, Wardill TJ, Sun Y, Pulver SR, Renninger SL, Baohan A, et al. Ultrasensitive fluorescent proteins for imaging neuronal activity. *Nature* (2013) 499 (7458):295–300. doi: 10.1038/nature12354

48. Cravo RM, Margatho LO, Osborne-Lawrence S, Donato J Jr., Atkin S, Bookout AL, et al. Characterization of kiss1 neurons using transgenic mouse models. *Neuroscience* (2011) 173:37–56. doi: 10.1016/j.neuroscience.2010.11.022

49. Madisen L, Garner AR, Shimaoka D, Chuong AS, Klapoetke NC, Li L, et al. Transgenic mice for intersectional targeting of neural sensors and effectors with high specificity and performance. *Neuron* (2015) 85(5):942–58. doi: 10.1016/j.neuron.2015.02.022

50. Cravo RM, Frazao R, Perello M, Osborne-Lawrence S, Williams KW, Zigman JM, et al. Leptin signaling in kiss1 neurons arises after pubertal development. *PloS One* (2013) 8(3):e58698. doi: 10.1371/journal.pone.0058698

51. Caligioni CS. Assessing reproductive status/stages in mice. *Curr Protoc Neurosci* (2009) Appendix 4:Appendix 4I. doi: 10.1002/0471142301.nsa04is48

52. Jamieson BB, Bouwer GT, Campbell RE, Piet R. Estrous cycle plasticity in the central clock output to kisspeptin neurons: implications for the preovulatory surge. *Endocrinology* (2021) 162(6):bqab071. doi: 10.1210/endocr/bqab071

53. Jamieson BB, Moore AM, Lohr DB, Thomas SX, Coolen LM, Lehman MN, et al. Prenatal androgen treatment impairs the suprachiasmatic nucleus arginine-vasopressin to kisspeptin neuron circuit in female mice. *Front Endocrinol (Lausanne)* (2022) 13:951344. doi: 10.3389/fendo.2022.951344

54. Edelstein A, Amodaj N, Hoover K, Vale R, Stuurman N. Computer control of microscopes using micromanager. *Curr Protoc Mol Biol* (2010) Chapter 14:Unit14 20. doi: 10.1002/0471142727.mb1420s92

55. Perkins KL. Cell-attached voltage-clamp and current-clamp recording and stimulation techniques in brain slices. *J Neurosci Methods* (2006) 154(1-2):1–18. doi: 10.1016/j.jneumeth.2006.02.010

56. Schindelin J, Arganda-Carreras I, Frise E, Kaynig V, Longair M, Pietzsch T, et al. Fiji: an open-source platform for biological-image analysis. *Nat Methods* (2012) 9 (7):676–82. doi: 10.1038/nmeth.2019

57. Narahashi T, Moore JW, Scott WR. Tetrodotoxin blockage of sodium conductance increase in lobster giant axons. *J Gen Physiol* (1964) 47(5):965–74. doi: 10.1085/jgp.47.5.965

58. Narahashi T. Tetrodotoxin: A brief history. *Proc Jpn Acad Ser B Phys Biol Sci* (2008) 84(5):147–54. doi: 10.2183/pjab.84.147

59. Piet R, Boehm U, Herbison AE. Estrous cycle plasticity in the hyperpolarization-activated current ih is mediated by circulating 17beta-estradiol in preoptic area kisspeptin neurons. *J Neurosci* (2013) 33(26):10828–39. doi: 10.1523/JNEUROSCI.1021-13.2013

60. Stephens SBZ, Kauffman AS. Estrogen regulation of the molecular phenotype and active translatome of avpv kisspeptin neurons. *Endocrinology* (2021) 162(9): bqab080. doi: 10.1210/endocr/bqab080

61. Han SY, Clarkson J, Piet R, Herbison AE. Optical approaches for interrogating neural circuits controlling hormone secretion. *Endocrinology* (2018) 159(11):3822–33. doi: 10.1210/en.2018-00594

62. Gocz B, Rumpler E, Sarvari M, Skrapits K, Takacs S, Farkas I, et al. Transcriptome profiling of kisspeptin neurons from the mouse arcuate nucleus reveals new mechanisms in estrogenic control of fertility. *Proc Natl Acad Sci U.S.A.* (2022) 119(27):e2113749119. doi: 10.1073/pnas.2113749119

63. de Croft S, Piet R, Mayer C, Mai O, Boehm U, Herbison AE. Spontaneous kisspeptin neuron firing in the adult mouse reveals marked sex and brain region differences but no support for a direct role in negative feedback. *Endocrinology* (2012) 153(11):5384–93. doi: 10.1210/en.2012-1616

64. Yeo SH, Kyle V, Morris PG, Jackman S, Sinnett-Smith LC, Schacker M, et al. Visualisation of kiss1 neurone distribution using a kiss1-cre transgenic mouse. *J Neuroendocrinol* (2016) 28(11):10.1111/jne.12435. doi: 10.1111/jne.12435

65. Sanz E, Bean JC, Palmiter RD, Quintana A, McKnight GS. Activation of kiss1 neurons in the preoptic hypothalamus stimulates testosterone synthesis in adult male mice. *bioRxiv* (2020). doi: 10.1101/2020.12.03.410878

66. Dorner G, Gotz F, Rohde W. On the evocability of a positive oestrogen feedback action on lh secretion in female and male rats. *Endokrinologie* (1975) 66(3):369–72.

67. Clarkson J, Herbison AE. Postnatal development of kisspeptin neurons in mouse hypothalamus; sexual dimorphism and projections to gonadotropin-releasing hormone neurons. *Endocrinology* (2006) 147(12):5817–25. doi: 10.1210/en.2006-0787

68. Kauffman AS, Gottsch ML, Roa J, Byquist AC, Crown A, Clifton DK, et al. Sexual differentiation of kiss1 gene expression in the brain of the rat. *Endocrinology* (2007) 148 (4):1774–83. doi: 10.1210/en.2006-1540

69. Poling MC, Luo EY, Kauffman AS. Sex differences in steroid receptor coexpression and circadian-timed activation of kisspeptin and rfrp-3 neurons may contribute to the sexually dimorphic basis of the lh surge. *Endocrinology* (2017) 158 (10):3565–78. doi: 10.1210/en.2017-00405

70. Kueng W, Wirz-Justice A, Menzi R, Chappuis-Arndt E. Regional brain variations of tryptophan, monoamines, monoamine oxidase activity, plasma free and total tryptophan during the estrous cycle of the rat. *Neuroendocrinology* (1976) 21 (4):289–96. doi: 10.1159/000122536

71. Cohen IR, Wise PM. Effects of estradiol on the diurnal rhythm of serotonin activity in microdissected brain areas of ovariectomized rats. *Endocrinology* (1988) 122 (6):2619–25. doi: 10.1210/endo-122-6-2619

72. Kitts CS, Johnson JH. Reversal by estrogen of the effect of dorsal raphe stimulation on release of lh but not prolactin. *J Neurosci Res* (1986) 15(2):253–9. doi: 10.1002/jnr.490150214

73. Petersen SL, Hartman RD, Barraclough CA. An analysis of serotonin secretion in hypothalamic regions based on 5-hydroxytryptophan accumulation or push-pull perfusion. Effects of mesencephalic raphe or locus coeruleus stimulation and correlated changes in plasma luteinizing hormone. *Brain Res* (1989) 495(1):9–19. doi: 10.1016/0006-8993(89)91213-4

74. Helena CV, Toporikova N, Kalil B, Stathopoulos AM, Pogrebna VV, Carolino RO, et al. Kndy neurons modulate the magnitude of the steroid-induced luteinizing hormone surges in ovariectomized rats. *Endocrinology* (2015) 156(11):4200–13. doi: 10.1210/en.2015-1070

75. Mittelman-Smith MA, Krajewski-Hall SJ, McMullen NT, Rance NE. Ablation of kndy neurons results in hypogonadotropic hypogonadism and amplifies the steroid-induced lh surge in female rats. *Endocrinology* (2016) 157(5):2015–27. doi: 10.1210/en.2015-1740

76. Hu MH, Li XF, McCausland B, Li SY, Gresham R, Kinsey-Jones JS, et al. Relative importance of the arcuate and anteroventral periventricular kisspeptin neurons in control of puberty and reproductive function in female rats. *Endocrinology* (2015) 156 (7):2619–31. doi: 10.1210/en.2014-1655

77. Lin XH, Lass G, Kong LS, Wang H, Li XF, Huang HF, et al. Optogenetic activation of arcuate kisspeptin neurons generates a luteinizing hormone surge-like secretion in an estradiol-dependent manner. *Front Endocrinol (Lausanne)* (2021) 12:775233. doi: 10.3389/fendo.2021.775233

78. Shen X, Liu Y, Li XF, Long H, Wang L, Lyu Q, et al. Optogenetic stimulation of kiss1(Arc) terminals in the avpv induces surge-like luteinizing hormone secretion *via* glutamate release in mice. *Front Endocrinol (Lausanne)* (2022) 13:1036235. doi: 10.3389/fendo.2022.1036235

79. Sullivan SD, Howard LC, Clayton AH, Moenter SM. Serotonergic activation rescues reproductive function in fasted mice: does serotonin mediate the metabolic effects of leptin on reproduction? *Biol Reprod* (2002) 66(6):1702–6. doi: 10.1095/biolreprod66.6.1702

80. Bhave VM, Nectow AR. The dorsal raphe nucleus in the control of energy balance. *Trends Neurosci* (2021) 44(12):946–60. doi: 10.1016/j.tins.2021.09.004

81. Morin LP, Allen CN. The circadian visual system, 2005. *Brain Res Rev* (2006) 51 (1):1–60. doi: 10.1016/j.brainresrev.2005.08.003

82. Lowry CA. Functional subsets of serotonergic neurones: implications for control of the hypothalamic-pituitary-adrenal axis. *J Neuroendocrinol* (2002) 14(11):911–23. doi: 10.1046/j.1365-2826.2002.00861.x

83. Myers B, Scheimann JR, Franco-Villanueva A, Herman JP. Ascending mechanisms of stress integration: implications for brainstem regulation of neuroendocrine and behavioral stress responses. *Neurosci Biobehav Rev* (2017) 74(Pt B):366–75. doi: 10.1016/j.neubiorev.2016.05.011